



Cite this: *Soft Matter*, 2019, 15, 4326

Rhombohedral trap for studying molecular oligomerization in membranes: application to daptomycin†

Ming-Tao Lee,^{ab} Wei-Chin Hung^c and Huey W. Huang^{id}*^d

A persistent problem in the studies of membrane-active peptides, including antimicrobial peptides and pathogenic amyloid peptides, is the lack of methods for investigating their molecular configurations in membranes. These peptides spontaneously bind to membranes from solutions, and often form oligomers that induce changes of membrane permeability. For antimicrobials, such actions appear to relate to the antimicrobial mechanisms, but for amyloid peptides, the oligomerization has been linked to neurodegenerative diseases. In many cases, no further understanding of such oligomerization has been achieved due to the lack of structural information. In this article, we will demonstrate a method of trapping such peptide oligomers in a rhombohedral (R) phase of lipid so that the oligomers can be subjected to 3D diffraction analysis. The conditions for forming the R phase and the electron density distribution in the rhombohedral unit cell provide information about peptide–lipid interactions and the molecular size of the trapped oligomer. Such information cannot be obtained from membranes in the planar configuration. For illustration, we apply this method to daptomycin, an FDA-approved antibiotic that attacks membranes containing phosphatidylglycerol, in the presence of calcium ions. We have successfully used the brominated phosphatidylglycerol to perform bromine-atom anomalous diffraction in the rhombohedral phase containing daptomycin and calcium ions. The preliminary results apparently exhibit diffraction data related to daptomycin oligomers. We believe that this method will also be applicable to the difficult problems related to amyloid peptides, such as amyloid beta of Alzheimer's disease.

Received 14th February 2019,
Accepted 24th April 2019

DOI: 10.1039/c9sm00323a

rsc.li/soft-matter-journal

Introduction

The difficulty of studying the structures of protein oligomers embedded in membranes is well known. In many such problems, even the size of the oligomers, or whether there is any regularity of oligomerization, is unknown. Yet, there are many known cases of peptide oligomerization in microbial membranes that is directly correlated to the peptide's antimicrobial actions. There are also cases of protein oligomerization in mammalian cell membranes that is correlated to diseases or toxicity. The lack of methods for analyzing protein oligomerization in membranes has been the bottleneck for many important problems in protein–membrane interactions. Here, we will describe a novel method for probing the oligomers that are spontaneously formed by various membrane-active peptides. We have in the recent past successfully

reconstructed the electron density structures of the barrel-stave pore and toroidal pore in membranes induced by alamethicin¹ and melittin,^{2,3} respectively. We will now extend this method to different types of oligomers.

The membrane pores formed by alamethicin or melittin were trapped in the unit cells of the rhombohedral (R) phase of brominated lipid. That made it possible to analyze their structures by anomalous X-ray diffraction. We have found that membranes containing peptide oligomers can be transformed into the R phase by osmotic stress. By trapping the peptide oligomers in the rhombohedral unit cells of lipid, we can subject the oligomers to X-ray diffraction analysis, both in the vertical (to membrane) direction and also in the horizontal direction—we call this method the rhombohedral trap for oligomers.

Oligomer problems are associated with some FDA (the U.S. Food and Drug Administration)-approved membrane-active antibiotics on the one hand and amyloid peptides related to neurodegenerative diseases on the other. Examples of antibiotics include daptomycin, a last resort antibiotic for the treatment of Gram-positive bacterial infections⁴ and amphotericin B that has served as the gold standard treatment for systemic fungal

^a National Synchrotron Radiation Research Center, Hsinchu, Taiwan

^b Department of Physics, National Central University, Jhongli, Taiwan

^c Department of Physics, R. O. C. Military Academy, Fengshan, Kaohsiung, Taiwan

^d Department of Physics and Astronomy, Rice University, Houston, TX, USA.

E-mail: hwhuang@rice.edu

† Electronic supplementary information (ESI) available. See DOI: 10.1039/c9sm00323a

infections, despite its toxicity.⁵ Examples of amyloid oligomers include the amyloid beta (Abeta) of Alzheimer's disease,^{6,7} prion protein fragment PrP 106–126^{8–10} and islet amyloid polypeptide (IAPP)^{11,12} that is associated with type 2 diabetes. In all of these cases, the oligomers are perceived to harm or kill cells by increasing the membrane permeability to ions without any evidence of discrete channel or pore formation or ion selectivity.^{4,6,8,10,13} We note that in the cases of amyloid peptides, the causes of amyloidosis remain controversial.⁶ One might call this class of peptides oligomer-forming membrane-active peptides, to distinguish them from the pore-forming host-defense antimicrobial peptides such as melittin, magainin or LL37.^{14–16} So far, there is very little understanding of these perceived oligomerizations. As a result, the mechanism(s) by which the drugs kill pathogens or how the amyloids harm cells is unknown.^{6,10}

The oligomers mentioned in the examples above are different from one another. The oligomerization of each membrane-active peptide or molecule is unique. It is not instructive to discuss their structural problems in general terms, although we believe that our proposed method is generally applicable to all types of oligomers. In the following, we will specifically discuss the oligomerization of daptomycin, as an example to demonstrate our new method.

Daptomycin is a lipopeptide antibiotic, notably active against multidrug-resistant Gram-positive pathogens, including methicillin-resistant *Staphylococcus aureus* (MRSA) and vancomycin-resistant *Enterococcus* (VRE).^{17–19} The evidence so far suggests that its main target is the bacterial cytoplasmic membrane, where daptomycin causes permeability to ions, leading to loss of membrane potential and cell death.^{4,17,18,20–22} The antibacterial activity of daptomycin is calcium-dependent²³ and correlates with the target membrane's content of phosphatidylglycerol (PG).²⁴ In lipid vesicle experiments, daptomycin causes ion permeability only in the vesicles containing PG and in the presence of calcium ions;^{17,25} exactly the same conditions were found to be necessary for daptomycin to be effective against bacteria. Recently, we have performed experiments on daptomycin with various types of lipid combinations, including DMPC/DMPG, DOPE/DOPG and DOPC/DOPG,^{26–28} and concluded that it is insensitive to the chain types of the lipid as long as PG is included.

One basic requirement for studying a membrane sample as a whole is the uniformity of the sample. For daptomycin studies, the sample must also include PG and calcium ions. In our previous studies, we were able to determine the stoichiometric ratio of the daptomycin/Ca²⁺/PG complex to be 2 : 3 : 2.²⁶ It is not a trivial matter to mix lipid and ions into a uniform, homogeneous sample. In the common method for the preparation of membrane samples with organic solvents,^{29,30} it is difficult to include ions. We will describe a new method of water-based preparation that results in well-aligned, homogeneous multilamellars of daptomycin, PC/PG, and Ca²⁺ mixtures, as proven by high orders of X-ray lamellar diffraction and a low mosaic. This method was used before for preparing multilamellars of lipopolysaccharides³¹ that do not dissolve in organic solvent. We have improved the water-based method

by shortening the time of preparation, which is important for varying the sample composition during the experiment.

In the following, we describe the oligomer problem of daptomycin, the method of sample preparation, and the rhombohedral trap method.

Experiment

Materials

Lipid 1,2-distearoyl(9,10-dibromo)-*sn*-glycero-3-phospho-(1'-*rac*-glycerol) [di18:0(9,10Br)PG, abbreviated as Br-DOPG in this paper] and 1,2-diphytanoyl-*sn*-glycero-3-phosphocholine (DPHPC) were purchased from Avanti Polar Lipids (Alabaster, AL). Calcium chloride (>98.0%) and other reagents of highest purity available were purchased from Sigma-Aldrich (St. Louis, MO).

Water-based multilamellar preparation

(1) Use lipid powder or evaporate organic solvent from lipid solution (lipids are typically supplied in chloroform).

(2) Add distilled water to the dry lipid. We found best results in the range of 160–320 μ L of water per mg of lipid.

(3) Sonicate the mixture into a suspension of small unilamellar vesicles (SUVs), for example, 60 min in an ultrasonicator at 15 W.

(4) Add daptomycin and Ca²⁺ (in the form of CaCl₂) in a 2 : 3 molar ratio to the SUV suspension, in which the PG to daptomycin molar ratio is ≥ 1 . Sonicate the suspension for an hour.

(5) Coat one to two bilayers of lipid on the cleaned surface of the substrate, either glass or silicon wafer. On glass, spread 0.001 mg of DOPG in organic solution onto a 18 \times 18 mm surface. Use neutral lipid on silicon wafer.

(6) Spread 0.5 mg of lipid in the SUV suspension on the 18 \times 18 mm substrate.

(7) Vacuum dry the sample at 40 $^{\circ}$ C for an hour.

(8) Then, keep the sample at 40 $^{\circ}$ C at saturated humidity before experiment.

Grazing-angle X-ray diffraction for the L to R phase transition

The experiment was performed at the beamline BL13A of the National Synchrotron Radiation Research Center (NSRRC, Hsin-Chu, Taiwan). The details of the experimental setup were described by Qian *et al.*¹ The multilamellar sample was positioned to be exposed to a beam of size 0.5 \times 0.3 mm² incident at $\sim 0.3^{\circ}$ relative to the substrate. Diffraction patterns were recorded on a Rayonix 165 detector (Rayonix, Evanston, IL) oriented vertically to the incident beam. A vacuumed beam path between the sample chamber and the detector was used to reduce air scattering. An aluminum attenuator was used to keep strong reflection orders from saturating the detector.

The sample was kept inside a humidity-temperature chamber.³² The chamber was covered by a double-layered insulating wall of mylar windows for the passage of X-ray. Between the double layers, a resistive heating coil maintained the surface temperature of the chamber above that of the sample so as to prevent water condensation on the windows.

The structural phase transitions were recorded for a series of samples at 30 °C by decreasing the relative humidity in the sample chamber starting from full hydration. The diffraction patterns on the detector were translated to the Q space following the procedure detailed in previous papers.^{32,33} The rhombohedral diffraction patterns are described by the set of reciprocal vectors $\mathbf{b}_1 = (1/a, 1/(\sqrt{3}a), -2/(3c))$, $\mathbf{b}_2 = (0, 2/(\sqrt{3}a), -1/(3c))$ and $\mathbf{b}_3 = (0, 0, 1/c)$ indexed by (h, k, l) , which correspond to the crystal axes $\mathbf{a}_1 = (a, 0, 0)$, $\mathbf{a}_2 = (-a/2, \sqrt{3}a/2, 0)$, and $\mathbf{a}_3 = (a/2, a/2\sqrt{3}, c)$.³² \mathbf{a}_1 , \mathbf{a}_2 , and \mathbf{a}_3 define the primitive unit cell, with the c axis normal to the lipid bilayers and, \mathbf{a}_1 and \mathbf{a}_2 the unit vectors of a hexagonal pattern on the plane of the bilayer. Equivalently, the rhombohedral lattice is described by the reciprocal vectors $\mathbf{B}_1 = (1/a, 1/(\sqrt{3}a), 0)$, $\mathbf{B}_2 = (0, 2/(\sqrt{3}a), 0)$, and $\mathbf{B}_3 = (0, 0, 1/(3c))$ indexed by (H, K, L) and the crystal axes $A_1 = (a, 0, 0)$, $A_2 = (-a/2, \sqrt{3}a/2, 0)$, and $A_3 = (0, 0, 3c)$. The cell defined by A_1 , A_2 , A_3 contains three primitive unit cells positioned at $(0, 0, 0)$, $(a/2, a/2\sqrt{3}, c)$, and $(0, a/\sqrt{3}, 2c)$.

Grazing-angle multiwavelength anomalous diffraction in the R phase

This experiment was performed for two samples with following lipid compositions: DPhPC/Br-DOPG (19:1) plus daptomycin/

Ca²⁺ (2:3) in the daptomycin/lipid ratio D/L = 1/40, and DPhPC/Br-DOPG (29:1) plus daptomycin/Ca²⁺ (2:3) in the daptomycin/lipid ratio D/L = 1/30, denoted as Dap/Ca/DPhPC:Br-DOPG (19:1) in the ratio 1/1.5/40 and Dap/Ca/DPhPC:Br-DOPG (29:1) in the ratio 1/1.5/30, respectively. Grazing angle bromine anomalous diffraction was performed at the beamline BL23A of the NSRRC with the same setup as that described above, except that the Rayonix CCD detector was replaced by a Pilatus-1MF detector (Dectris, Baden-Dättwil, Switzerland). The initial steps included measuring the wavelength dependence of the detectors and the absorption spectrum of bromine,³⁴ from which the real f'_λ and imaginary f''_λ parts of the bromine atom's anomalous scattering factor were obtained from the measured absorption spectra.³⁴ The numerical values of f'_λ and f''_λ of bromine have been measured previously, and are available in a graph³⁵ and a table.³⁴ The energy of the bromine K-edge is 13.474 keV. Ten sub-edge X-ray energies were chosen such that the values of f'_λ at successive energies differ by $\Delta f'_\lambda = 0.5$ in the unit of electron (Table 1 of ref. 34). It is important to note that the grazing-angle diffraction was completed by a combination of two separate scans: a grazing angle off-specular scan for all (H, K, L) except for $(0, 0, L)$, and a $\theta-2\theta$ scan for $(0, 0, L)$ peaks.³² Then, these two different scans were normalized to each other.³²

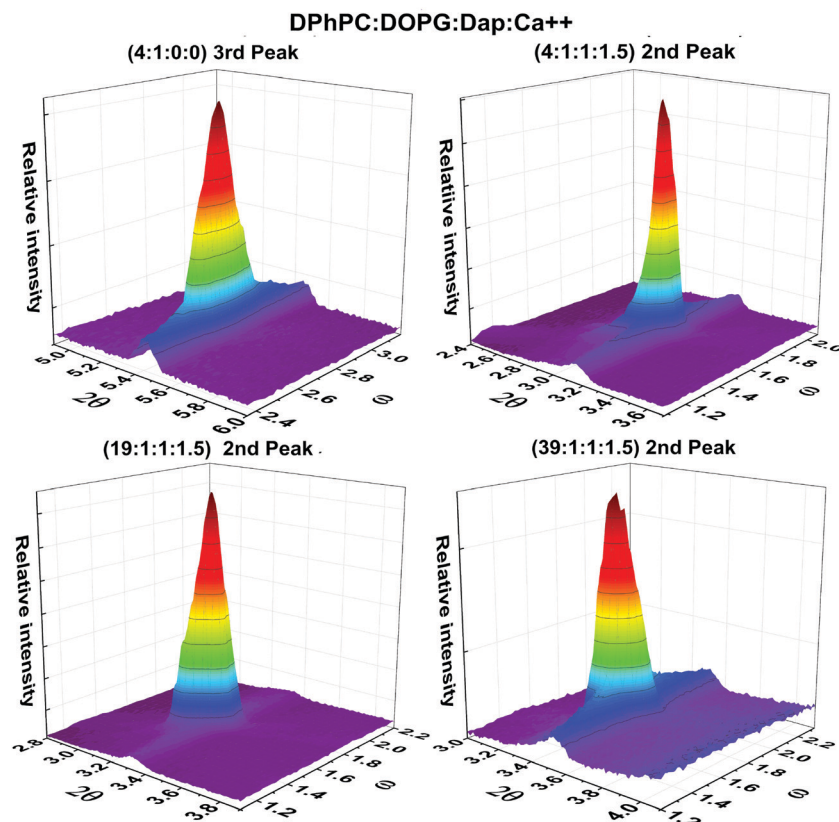


Fig. 1 Two dimensional rocking (ω , 2θ) scan for four different compositions of DPhPC, DOPG, daptomycin and CaCl₂—the molar ratios are indicated on the labels. The purpose was to test the water-based multilamellar sample preparation. In all cases, the mosaic spread is about 0.2 deg. full width at half maximum.

Results

1. Water-based multilamellar sample preparation

A series of samples based on the lipid composition DPhPC/Br-DOPG at various ratios, plus daptomycin/ Ca^{2+} always in a 2:3 ratio, with different daptomycin to PG ratios was prepared, according to the procedure described, as a test for the method of sample preparation. In all cases, the ratio of PG to daptomycin was equal or greater than one. The choices are based on the stoichiometric ratios of the daptomycin/ Ca^{2+} /PG complex that is explained below.

The procedure for preparing multilamellar samples was based on our previous experience of preparing similar samples of lipopolysaccharides,³¹ which are not soluble in organic solvent. Here, we have tested several variations of the procedure in order to shorten the time of preparation. The steps given in the Experimental section are our optimized version. The resulting multilamellar samples appeared to have uniform thickness with a smooth surface. Lamellar diffraction showed 6 or more Bragg peaks at low humidity ($\sim 90\%$ RH) and appeared to be hydration-saturated at $\sim 97\%$ RH due to the presence of ions in the samples. Two dimensional ω - 2θ scans consistently showed a mosaic spread of <0.2 deg. full width at half maximum, indicating excellent alignment and uniformity (Fig. 1).

2. Rhombohedral phase

The lipid phases are easily identifiable by grazing angle diffraction from multilamellar samples. Unlike powder diffraction, which produces rings of different radii in Q , grazing angle diffraction from lipid phases appears in a pattern of peaks on a 2D area detector oriented perpendicular to the incident beam. The patterns for the R phase and HII phase have been identified previously³⁶ (reproduced in Fig. S1 for convenience, ESI[†]). In fact, one can identify them from a few strong peaks (Fig. 2). The phase transitions in pure lipids or lipid composites have been studied in detail.^{36–38} It is important to note that the phase boundaries can be complicated³⁸ as neighboring phases tend to coexist. For our purpose, it is important to find out if a pure R phase of our samples is obtainable.

Daptomycin/ Ca^{2+} (2:3) mixed with DPhPC/Br-DOPG (19:1) bilayers in various daptomycin to total lipid ratios (abbreviated as D/L) was observed for its lipid phase behavior by using

grazing angle X-ray diffraction. The sample was housed in a temperature/humidity chamber³² maintained at 30°C . Applying osmotic stress to the lipid by lowering the water vapor pressure from $\sim 100\%$ RH, we found that the lipids transformed from the lamellar (L_α abbreviated by L) phase to the rhombohedral (R) phase and then to the inverted hexagonal (HII abbreviated as H) phase. Fig. 2 shows the phase transitions from the L phase to the R phase, and at lower RH, the appearance of the coexisting H phase. In our case, the transition from L to R is clean, but H first appears to coexist with R. Near the L–R phase boundary, the contamination of the H phase is absent or minimal.

Fig. 3 shows the RH value of the L–R phase boundary for different daptomycin to total lipid D/L ratios. The result indicates that the samples with D/L between 1/40 and 1/30 require the least osmotic stress to transform from L to R.

3. Anomalous diffraction

Multiwavelength anomalous grazing-angle diffraction is a laborious experiment. Each off-specular scan is coupled with a θ - 2θ scan for $(0, 0, L)$ peaks.³⁴ The same procedure was repeated at ten different X-ray energies below the Br K-edge. For each diffraction peak, the background signal needs to be removed with care by matching with the far away background.³² The peak intensity was then integrated to give the absolute square of the amplitude $|F_\lambda(H, K, L)|$. (H, K, L) indices of the diffraction peaks (shown in Fig. 4) can be found in ref. 32. All together, 16 independent Bragg peaks were detected for each of the two samples: Dap/Ca/DPhPC: Br-DOPC (29:1) in daptomycin/lipid ratio D/L = 1/40, and Dap/Ca/DPhPC: Br-DOPC (19:1) in daptomycin/lipid ratio D/L = 1/30. The symmetry related peaks are counted as one peak.

The method of multiwavelength anomalous diffraction has been described in previous work.^{34,35} The diffraction amplitude F_λ from a unit cell containing bromine atoms with atomic scattering factor $f = f^n + f'_\lambda + if''_\lambda$ is written as

$$F_\lambda = \sum_j f_j^n \exp(i\mathbf{Q} \cdot \mathbf{r}_j) + \sum_k (f^n + f'_\lambda + if''_\lambda) \exp(i\mathbf{Q} \cdot \mathbf{r}_k) \quad (1)$$

$$= F_0 + \frac{f'_\lambda + if''_\lambda}{f^n} F_2$$

where f^n is the normal Br atomic scattering factor, and f'_λ and f''_λ are the real and imaginary parts of the anomalous scattering

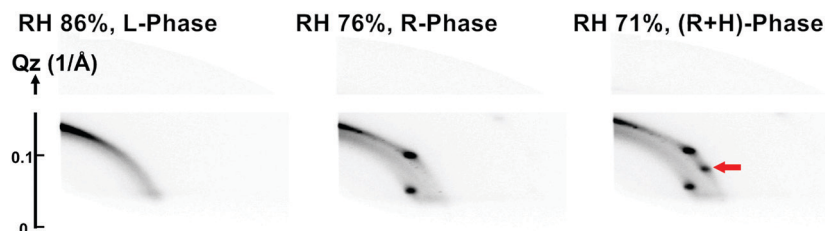


Fig. 2 The detector image of grazing angle diffraction. The phases can be identified by a few strongest peaks.³⁸ For this sample, Dap/Ca/DPhPC: Br-DOPG (29:1) at 1/1.5/30, the lamellar (L_α) phase gave very strong lamellar peaks on the Q_z axis. The powder ring shown in this image is negligible compared to the lamellar peaks. In this image, the lamellar peaks were blocked and the detector intensity was magnified to show the side peaks. The R phase first appears at RH 76% (identified by the two peaks at $H = 0, K = 1, L = 1$ and $H = 1, K = 0, L = 2$ ³²). The Hii phase (identified by the peak indicated by the red arrow)³⁵ appears at RH 71% coexisting with the R phase.

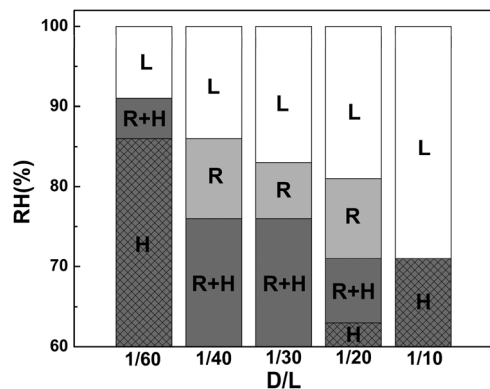


Fig. 3 Phase diagram of the mixtures of Dap/Ca (2:3) and DPhPC: Br-DOPG (19:1) or (29:1) at various daptomycin to total lipid D/L ratios. L for lamellar, R for rhombohedral and H for hexagonal phase.

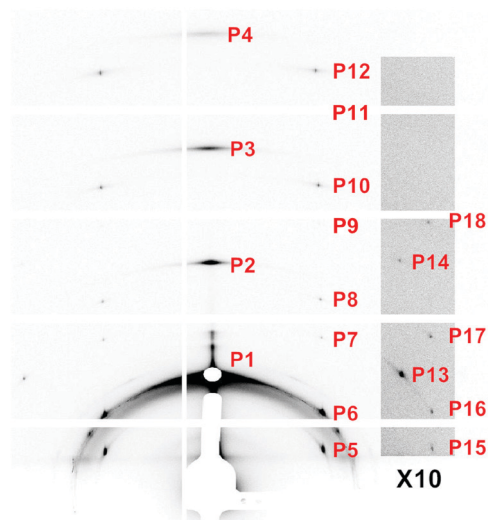


Fig. 4 The diffraction peaks of Dap/Ca/DPhPC:Br-DOPG (19:1) in the ratio 1/1.5/40. This off specular diffraction and the θ - 2θ scan of the lamellar peaks for P1–P4 were measured at ten wavelengths with energies just below the Br K-edge. The vertical and horizontal white lines are the gaps of the Pilatus detector. The (H, K, L) indices of the peaks are available in ref. 32.

factor. F_0 is the normal diffraction amplitude of the whole system and F_2 is the normal diffraction amplitude of the Br atoms alone. From the way the samples were prepared, we will assume that the unit cell is on average centrosymmetric, so that both F_0 and F_2 are real (rather than complex) quantities and their phases are the signs of the amplitudes. (Note that this centrosymmetry assumption will be validated by the data.) Then, we have $|F_\lambda|^2 = [F_0 + (f'_\lambda/f^n)F_2]^2 + (f''_\lambda/f^n)^2 F_2^2$. From the numerical values³⁴ of f'_λ and f''_λ , at energies below the absorption edge, f''_λ is about 10% of $|f'_\lambda|$, therefore the second term is about 1% of the first term. Consequently, we obtain the approximate relation

$$|F_\lambda| \approx \pm \left(F_0 - \frac{|f'_\lambda|}{f^n} F_2 \right) \quad (2)$$

For each sample, the diffraction amplitude F_λ was measured at ten sub-edge X-ray energies. We plotted $|F_\lambda|$ against $|f'_\lambda|/f^n$ for each peak (Fig. 5). The data appear to satisfy a linear relation (*i.e.*, approximate fit to a straight line). Since the linear relation eqn (2) is the result of the centrosymmetry assumption, we see that this assumption is justified by the results shown in Fig. 5. In each plot, we fitted the data with a straight line; the intercept of the fitted line gives $|F_0|$; the magnitude of the slope gives $|F_2|$; and the sign of the slope gives the sign of $-F_0/F_2$ (Table 1).

Discussion and conclusions

1. Daptomycin

Daptomycin belongs to a family of cyclic peptides with a hydrocarbon chain acylated to its N-terminal (the first 10 amino acids in a ring, an *n*-decanoyl chain acylated to the 13th amino acid; see Fig. 1 of ref. 26 reproduced in Fig. S2 for convenience, ESI[†]). Its antibiotic function is calcium-dependent and specific to membranes containing phosphatidylglycerol (PG). For years, the mode of action of daptomycin has been assumed to be causing membrane permeability to ions that leads to the loss of membrane potential and cell death.^{4,17,18,20,21,24,39–45} Thus, the common hypothesis has been the formation of ion channels by daptomycin.^{4,45–47} However, recently, Müller *et al.*²² carried out an *in vivo* study on *B. subtilis* membranes using a combination of proteomics, ionomics, and fluorescence microscopy assays. They found that daptomycin selectively clusters in fluid membrane domains and causes dislocation of several peripheral membrane proteins with the consequence of depolarization of the membrane potential and cell envelope stress, but the evidence excluded the possibility of ion channels.

This and other *in vivo* studies^{4,22,45} implicate no direct daptomycin–protein interactions. Instead, the mutations that alter susceptibility to daptomycin appear to directly affect the membrane lipid composition,^{24,41–44} indicating that the bacterial membranes are the central target for the action of daptomycin.^{4,17,18,20,21,24,39–44} This makes it reasonable to look for the mechanism by which daptomycin alters the membrane permeability in model lipid membranes. Indeed, fluorescence resonance energy transfer (FRET) experiments detected oligomerization of daptomycin in the presence of PG-containing membranes and calcium ions.^{48–50} Our recent giant unilamellar vesicle (GUV) experiment^{27,28} demonstrated that the membrane exposed to daptomycin increased its total membrane area, directly indicating daptomycin insertion into the membrane, and subsequent ions leakage into the GUV while the dye molecules encapsulated inside the GUV did not leak out.²⁸ Thus, the central question is how does daptomycin induce ion permeability of the membrane?

In a separate experiment,²⁶ we found that the system consisting of three components, *i.e.*, daptomycin, calcium ions, and PG-containing membranes, as a function of their concentrations, exhibits only two basic CD spectra (see Fig. 3 of ref. 26, reproduced in Fig. S3 for convenience, ESI[†]). The state of monomeric daptomycin (proven by small angle X-ray scattering) in the absence of

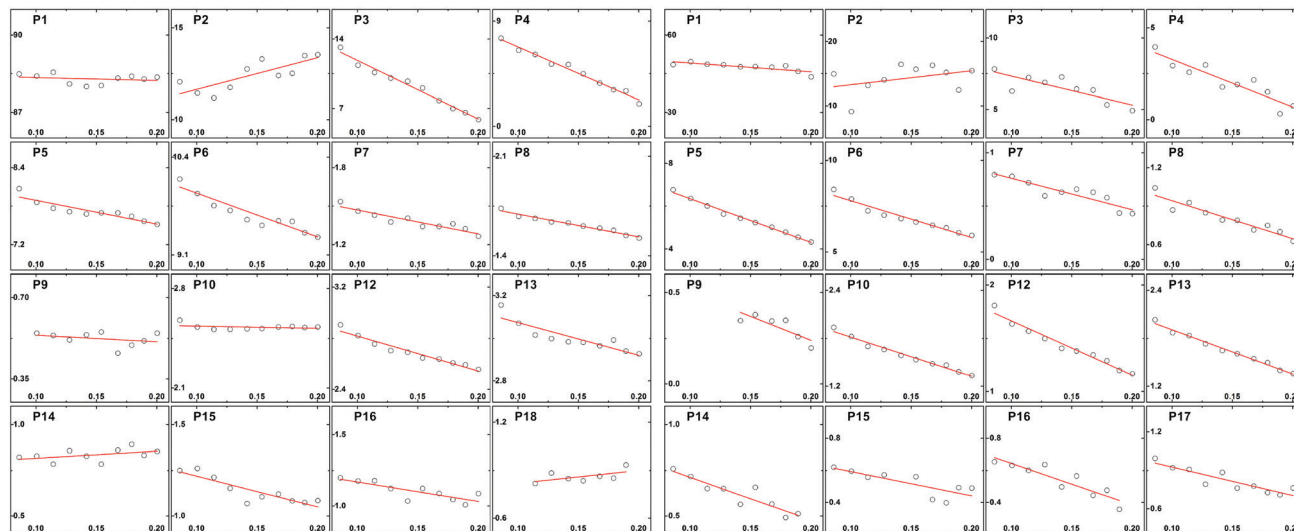


Fig. 5 Each box represents a peak shown in Fig. 4, in which the vertical coordinate $|F_x|$ is plotted vs. the horizontal coordinate $\frac{|f_x'|}{f^n}$ at ten wavelengths (see eqn (2)). The left panel is for the sample Dap/Ca²⁺/DPhPC : Br-DOPG (19 : 1) at 1/1.5 : 40 ratio, abbreviated as D/L = 1/40. The right panel is for the sample Dap/Ca²⁺/DPhPC : Br-DOPG (29 : 1) at 1/1.5/30 ratio, abbreviated as D/L = 1/30.

Table 1 Results of multiwavelength Br-anomalous diffraction analysis. The peak numbers are identified in Fig. 4

Peak no.	Dap/Ca/DPhPC : Br-DOPG (19 : 1) 1/1.5/40			Dap/Ca/DPhPC : Br-DOPG (29 : 1) 1/1.5/30		
	$ F_2 $	$ F_0 $	$-F_0/F_2$	$ F_2 $	$ F_0 $	$-F_0/F_2$
P1	1.0807	88.4523	-81.85	34.3426	52.5816	-1.53
P2	17.2331	9.9226	0.58	21.7213	11.1021	0.51
P3	59.2055	17.7647	-0.30	20.2545	9.3598	-0.41
P4	45.2843	11.3168	-0.25	25.8895	5.8672	-0.23
P5	3.6925	8.2598	-2.24	20.3963	8.3891	-0.41
P6	5.7964	10.5024	-1.81	20.0569	9.8040	-0.49
P7	1.8580	1.6559	-0.89	2.9393	1.0547	-0.36
P8	1.5985	1.8542	-1.16	2.9638	1.2392	-0.42
P9	0.2800	0.5665	-2.02	2.6078	0.7613	-0.29
P10	0.1565	2.5518	-16.31	4.8928	2.3055	-0.47
P11	*	*	*	*	*	*
P12	2.7280	3.0910	-1.13	5.0840	2.1726	-0.43
P13	2.5311	3.2270	-2.11	5.5252	2.4599	-0.45
P14	0.3871	0.7777	2.01	2.3468	0.9476	-0.40
P15	1.6863	1.3878	-0.82	1.5129	0.7448	-0.49
P16	1.3740	1.3072	-0.95	2.5905	0.9035	-0.35
P17	*	*	*	2.2205	1.1491	-0.52
P18	0.8038	0.7396	0.92	*	*	*

* Indicates that the amplitude is too small to be measured accurately.

one or two other components has a unique CD spectrum called the A state. This is the non-binding state of daptomycin. Daptomycin with excessive calcium and PG has another distinct CD spectrum called the B state. This is the membrane-bound state of daptomycin. Under all other conditions, the CD of the system is a linear combination of A and B.²⁶ Furthermore, we were able to establish the stoichiometric ratios of daptomycin/Ca²⁺/PG in the B state to be 2 : 3 : 2, assuming that only the PG in the outer layer of the vesicles is available for reaction.²⁶ (The ratios would be 2 : 3 : 4 if all PG on both sides of the vesicles is available for reaction.²⁶) Since the experiment was performed with pre-formed small unilamellar vesicles (SUVs) mixed into a daptomycin and CaCl₂

solution, we believe that 2 : 3 : 2 is the correct ratio. In the present study, we kept the ratio between daptomycin and Ca²⁺ 2 : 3, and the PG to daptomycin ratio ≥ 1 .

2. Water-based lamellar preparation

For experiments that measure the properties of the whole lamellar sample, such as X-ray and neutron diffraction and solid state NMR, the uniformity and homogeneity of the sample are paramount. We found that the water-based method produces excellent multilamellar samples containing ions, which are difficult to prepare by the conventional method based on organic solvent.^{29,30}

We observed an interesting phenomenon during step 4 of the sample preparation when calcium and daptomycin were mixed into the lipid SUV suspension. If CaCl₂ was added to the suspension first, the suspension became milky indicating strong light scattering as a result of vesicle aggregation. This was expected and has been observed in many past experiments, *e.g.*, in a vesicle fusion experiment.⁵¹ However, the suspension became clear when daptomycin was added. On the other hand, if the sequence of addition of CaCl₂ and daptomycin was reversed, the suspension remained clear throughout the process. To the best of our knowledge, this apparent demonstration of Ca²⁺ forming complexes with daptomycin in the presence of PC/PG vesicles has never been reported before. According to the stoichiometric ratio, this “milky to clear” phenomenon should occur only if the added daptomycin to Ca²⁺ ratio is equal or greater than 2 : 3.

3. Rhombohedral trap

The discovery of the rhombohedral (R) phase of lipids³⁷ led to the discovery of a long-spectulated membrane fusion intermediate state called stalk.³⁶ Subsequently, we found that lipids containing alamethicin or melittin (or melittin-like peptides²) also formed

the R phase. The electron distributions in these R phases revealed the structures of the barrel-stave pore¹ and the toroidal pore^{2,3} for the first time. In these cases, we knew from other independent experiments the threshold concentration (the peptide to lipid ratio) for alamethicin and melittin to form pores. But what is the concentration for daptomycin in the membrane to form oligomers? The peptide concentration in membrane is one of the unknowns in the problem of peptide oligomerization. For this experiment, we tested the samples with the daptomycin to lipid ratio varying from 1/60 to 1/10 (Fig. 3).

In the R phase, the lipid–daptomycin–Ca²⁺ mixture forms a hexagonal array in each lipid bilayer; and the hexagons of neighboring layers stack up in a face-centered cubic fashion (also called ABCABC packing).³⁷ Each unit cell is a hexagonal prism of one lipid bilayer. Due to the symmetry, the daptomycin oligomers must be at the center of the hexagonal unit cell. The unit cells in the R phase are all identical, otherwise they would not produce a crystalline diffraction. Besides the apparent advantage that the R phase allows 3D diffraction analysis of the trapped oligomers, the formation of rhombohedral unit cells containing oligomers opens new ways for probing the lipid–oligomer interaction.

(1) The formation of the R phase in which each unit cell contains the same oligomer implies the regularity of daptomycin oligomerization, *i.e.*, the oligomers are all of the same size. We want to stress that this regularity of oligomerization has never been known. Throughout more than two decades of research on daptomycin, no definitive oligomer or complex of daptomycin has been deduced based on its chemical structure (Fig. S2, ESI†). Even the stoichiometric ratios²⁶ do not imply a definitive size of oligomerization. We now know for the first time that daptomycin forms a definitive oligomer trapped in each rhombohedral unit cell.

(2) The RH value for the phase transition from the L phase to the R phase depends on the daptomycin to lipid ratio D/L in the sample. The higher the RH value, the less osmotic stress needed to cause the phase transition. Samples from D/L = 1/40 to 1/30 require the least osmotic stress implying that the R phase is most readily formed in this range of D/L. Accordingly, we applied anomalous diffraction to two samples: Dap/Ca²⁺/DPhPC : Br-DOPG (19 : 1) at 1/1.5/40 ratio and Dap/Ca²⁺/DPhPC : Br-DOPG (29 : 1) at 1/1.5/30 ratio. They will be abbreviated as D/L = 1/40 and D/L = 1/30 in the following discussion.

(3) Biologically produced compounds have very minor differences in electron densities. It is difficult to measure the electron density distribution of individual compounds unless the sample is truly crystalline. Membranes do not crystallize. Heavy atom labeling (or deuteration for neutron diffraction) is the only way to produce electron density contrast in membranes. In our case, bromine labeling on lipids is probably chemically the easiest (although expensive). For the current investigation, we used Br-DOPG. In D/L = 1/40, the number of PGs per lipid is 1/20 and the number of daptomycin per lipid is 1/40. There are 2 PGs per daptomycin. In D/L = 1/30, there is one PG per daptomycin.

In Table 1, F_0 is the normal diffraction amplitude of the whole system and F_2 is the normal diffraction amplitude of the

Br atoms alone. If we inspect the relative magnitudes of the amplitudes within each sample, the relative magnitudes of F_0 from peak 1 to 16 are similar between two samples. This is to be expected. Daptomycin and PG are minorities in each sample, therefore F_0 is basically the amplitude of the DPhPC bilayer in the rhombohedral unit cell. On the other hand, the relative magnitudes of F_2 within each sample are very different between the two samples. The side peaks (P5–P16), with H and K not both zero, are much stronger relative to the central lamellar peaks (P1–P4) in D/L = 1/30 compared to D/L = 1/40. This implies that the distribution of PG is more concentrated toward the center in D/L = 1/30 than in D/L = 1/40. Independently, we can reasonably assume that daptomycin in the hexagonal unit cell is concentrated at the center due to symmetry. Given that the stoichiometric ratio of daptomycin to PG is 1 : 1, PGs must also concentrate at the center in D/L = 1/30. In contrast, in D/L = 1/40, there are 2 PGs per daptomycin, therefore there are extra non-binding PGs not concentrated at the center. This is consistent with the principle of diffraction, *i.e.*, diffraction is the Fourier transform of the real space electron distribution, therefore the narrower the real space distribution, the wider the diffraction spreads in Q space.

This agreement between the known stoichiometry and the result of anomalous diffraction is proof that the method of rhombohedral trap is providing structural information about the daptomycin oligomer. Ultimately, we must resolve the electron density distribution from the diffraction data. To do so, we must solve the phase problem. Although we solved the phase problem in one case by the swelling method,^{32,36} solving the diffraction phases is in general difficult. A more practical approach is model fitting the magnitudes of the peak amplitudes, because there are only 16 amplitudes and each amplitude is either positive or negative. To that end, more complimentary sets of data will produce more restricting models. Here, for example, we can use the combination of brominated PC and plain PG to perform anomalous diffraction for a complimentary data set where the lipid surrounding the daptomycin oligomer is highlighted by bromine. In fact, this was how the structures of the barrel-stave pore¹ and toroidal pores³ were solved.

The preliminary data presented above strongly suggest the possibility of measuring the size of the oligomers and determining the variability of oligomerization with sample composition. Further studies should reveal the resolution limit of this method of rhombohedral trap.

Conflicts of interest

There are no conflicts to declare.

Acknowledgements

This work was supported by Taiwan research grants MOST 107-2112-M-213-006 (to M. T. L.) and MOST 107-2112-M-145-001 (to W. C. H.) and by NIH (US) Grant GM55203 (to H. W. H.).

References

- 1 S. Qian, W. Wang, L. Yang and H. W. Huang, *Biophys. J.*, 2008, **94**, 3512–3522.
- 2 S. Qian, W. Wang, L. Yang and H. W. Huang, *Proc. Natl. Acad. Sci. U. S. A.*, 2008, **105**, 17379–17383.
- 3 M. T. Lee, T. L. Sun, W. C. Hung and H. W. Huang, *Proc. Natl. Acad. Sci. U. S. A.*, 2013, **110**, 14243–14248.
- 4 J. A. Silverman, N. G. Perlmutter and H. M. Shapiro, *Antimicrob. Agents Chemother.*, 2003, **47**, 2538–2544.
- 5 T. M. Anderson, M. C. Clay, A. G. Cioffi, K. A. Diaz, G. S. Hisao, M. D. Tuttle, A. J. Nieuwkoop, G. Comellas, N. Maryum, S. Wang, B. E. Uno, E. L. Wildeman, T. Gonen, C. M. Rienstra and M. D. Burke, *Nat. Chem. Biol.*, 2014, **10**, 400–406.
- 6 H. A. Lashuel and P. T. Lansbury, Jr., *Q. Rev. Biophys.*, 2006, **39**, 167–201.
- 7 E. Terzi, G. Holzemann and J. Seelig, *Biochemistry*, 1997, **36**, 14845–14852.
- 8 R. Kaye, E. Head, J. L. Thompson, T. M. McIntire, S. C. Milton, C. W. Cotman and C. G. Glabe, *Science*, 2003, **300**, 486–489.
- 9 Y. Sun, W. C. Hung, M. T. Lee and H. W. Huang, *Biochim. Biophys. Acta, Biomembr.*, 2015, **1848**, 2422–2429.
- 10 R. Kaye, Y. Sokolov, B. Edmonds, T. M. McIntire, S. C. Milton, J. E. Hall and C. G. Glabe, *J. Biol. Chem.*, 2004, **279**, 46363–46366.
- 11 C. C. Lee, Y. Sun and H. W. Huang, *Biophys. J.*, 2012, **102**, 1059–1068.
- 12 S. A. Jayasinghe and R. Langen, *Biochim. Biophys. Acta*, 2007, **1768**, 2002–2009.
- 13 L. N. Ermishkin, K. M. Kasumov and V. M. Potzeluyev, *Nature*, 1976, **262**, 698–699.
- 14 M. Zasloff, *Nature*, 2002, **415**, 389–395.
- 15 H. W. Huang and N. E. Charron, *Q. Rev. Biophys.*, 2017, **50**, e10.
- 16 C. C. Lee, Y. Sun, S. Qian and H. W. Huang, *Biophys. J.*, 2011, **100**, 1688–1696.
- 17 J. Pogliano, N. Pogliano and J. A. Silverman, *J. Bacteriol.*, 2012, **194**, 4494–4504.
- 18 P. Cottagnoud, *Swiss Med. Wkly.*, 2008, **138**, 93–99.
- 19 C. Vilhena and A. Bettencourt, *Mini-Rev. Med. Chem.*, 2012, **12**, 202–209.
- 20 C. T. Mascio, J. D. Alder and J. A. Silverman, *Antimicrob. Agents Chemother.*, 2007, **51**, 4255–4260.
- 21 J. K. Hobbs, K. Miller, A. J. O'Neill and I. Chopra, *J. Antimicrob. Chemother.*, 2008, **62**, 1003–1008.
- 22 A. Muller, M. Wenzel, H. Strahl, F. Grein, T. N. Saaki, B. Kohl, T. Siersma, J. E. Bandow, H. G. Sahl, T. Schneider and L. W. Hamoen, *Proc. Natl. Acad. Sci. U. S. A.*, 2016, **113**, E7077–E7086.
- 23 A. L. Barry, P. C. Fuchs and S. D. Brown, *Antimicrob. Agents Chemother.*, 2001, **45**, 1919–1922.
- 24 A. B. Hachmann, E. Sevim, A. Gaballa, D. L. Popham, H. Antelmann and J. D. Helmann, *Antimicrob. Agents Chemother.*, 2011, **55**, 4326–4337.
- 25 T. Zhang, J. K. Muraih, B. MacCormick, J. Silverman and M. Palmer, *Biochim. Biophys. Acta*, 2014, **1838**, 2425–2430.
- 26 M. T. Lee, W. C. Hung, M. H. Hsieh, H. Chen, Y. Y. Chang and H. W. Huang, *Biophys. J.*, 2017, **113**, 82–90.
- 27 Y. F. Chen, T. L. Sun, Y. Sun and H. W. Huang, *Biochemistry*, 2014, **53**, 5384–5392.
- 28 M. T. Lee, P. Y. Yang, N. E. Charron, M. H. Hsieh, Y. Y. Chang and H. W. Huang, *Biochemistry*, 2018, **57**, 5629–5639.
- 29 Y. K. Levine and M. H. Wilkins, *Nature (London), New Biol.*, 1971, **230**, 69–72.
- 30 N. P. Franks and W. R. Lieb, *J. Mol. Biol.*, 1979, **133**, 469–500.
- 31 L. Ding, L. Yang, T. M. Weiss, A. J. Waring, R. I. Lehrer and H. W. Huang, *Biochemistry*, 2003, **42**, 12251–12259.
- 32 L. Yang and H. W. Huang, *Biophys. J.*, 2003, **84**, 1808–1817.
- 33 L. Ding, T. M. Weiss, G. Fragneto, W. Liu, L. Yang and H. W. Huang, *Langmuir*, 2005, **21**, 203–210.
- 34 W. Wang, D. Pan, Y. Song, W. Liu, L. Yang and H. Huang, *Biophys. J.*, 2006, **91**, 736–743.
- 35 D. Pan, W. Wangchen, W. Liu, L. Yang and H. W. Huang, *J. Am. Chem. Soc.*, 2006, **128**, 3800–3807.
- 36 L. Yang and H. W. Huang, *Science*, 2002, **297**, 1877–1879.
- 37 L. Yang, T. M. Weiss and H. W. Huang, *Biophys. J.*, 2000, **79**, 2002–2009.
- 38 L. Yang, L. Ding and H. W. Huang, *Biochemistry*, 2003, **42**, 6631–6635.
- 39 N. E. Allen, J. N. Hobbs and W. E. Alborn, Jr., *Antimicrob. Agents Chemother.*, 1987, **31**, 1093–1099.
- 40 N. Cotroneo, R. Harris, N. Perlmutter, T. Beveridge and J. A. Silverman, *Antimicrob. Agents Chemother.*, 2008, **52**, 2223–2225.
- 41 C. A. Arias, D. Panesso, D. M. McGrath, X. Qin, M. F. Mojica, C. Miller, L. Diaz, T. T. Tran, S. Rincon, E. M. Barbu, J. Reyes, J. H. Roh, E. Lobos, E. Sodergren, R. Pasqualini, W. Arap, J. P. Quinn, Y. Shamoo, B. E. Murray and G. M. Weinstock, *N. Engl. J. Med.*, 2011, **365**, 892–900.
- 42 L. Friedman, J. D. Alder and J. A. Silverman, *Antimicrob. Agents Chemother.*, 2006, **50**, 2137–2145.
- 43 K. L. Palmer, A. Daniel, C. Hardy, J. Silverman and M. S. Gilmore, *Antimicrob. Agents Chemother.*, 2011, **55**, 3345–3356.
- 44 M. Davlieva, W. Zhang, C. A. Arias and Y. Shamoo, *Antimicrob. Agents Chemother.*, 2013, **57**, 289–296.
- 45 W. E. Alborn, Jr., N. E. Allen and D. A. Preston, *Antimicrob. Agents Chemother.*, 1991, **35**, 2282–2287.
- 46 S. K. Straus and R. E. Hancock, *Biochim. Biophys. Acta*, 2006, **1758**, 1215–1223.
- 47 S. D. Taylor and M. Palmer, *Bioorg. Med. Chem.*, 2016, **24**, 6253–6268.
- 48 J. K. Muraih, A. Pearson, J. Silverman and M. Palmer, *Biochim. Biophys. Acta*, 2011, **1808**, 1154–1160.
- 49 J. K. Muraih, J. Harris, S. D. Taylor and M. Palmer, *Biochim. Biophys. Acta*, 2012, **1818**, 673–678.
- 50 J. K. Muraih and M. Palmer, *Biochim. Biophys. Acta*, 2012, **1818**, 1642–1647.
- 51 H. Ellens, D. P. Siegel, D. Alford, P. L. Yeagle, L. Boni, L. J. Lis, P. J. Quinn and J. Bentz, *Biochemistry*, 1989, **28**, 3692–3703.

Supplemental Information

Rhombohedral Trap for Studying Molecular Oligomerization in Membranes: Application to Daptomycin

Ming-Tao Lee^{1,2}, Wei-Chin Hung³ and Huey W. Huang^{*4}

Fig S1. Grazing angle diffraction patterns of the lamellar (L), rhombohedral (R) and hexagonal (H) phases (reproduced from ref 36 for convenience).

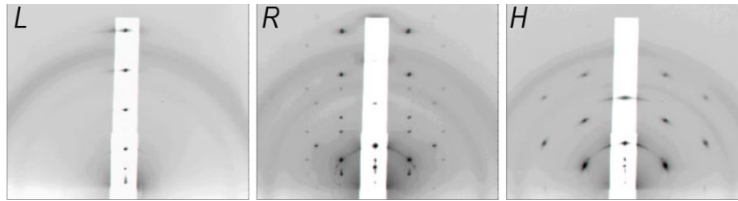


Fig S2 Structural formula of daptomycin with CPKTM space filling atomic models. Two sides of the CPK model of daptomycin are shown along with lipid DOPG. Their sizes are in proportion to each other (reproduced from ref. 26).

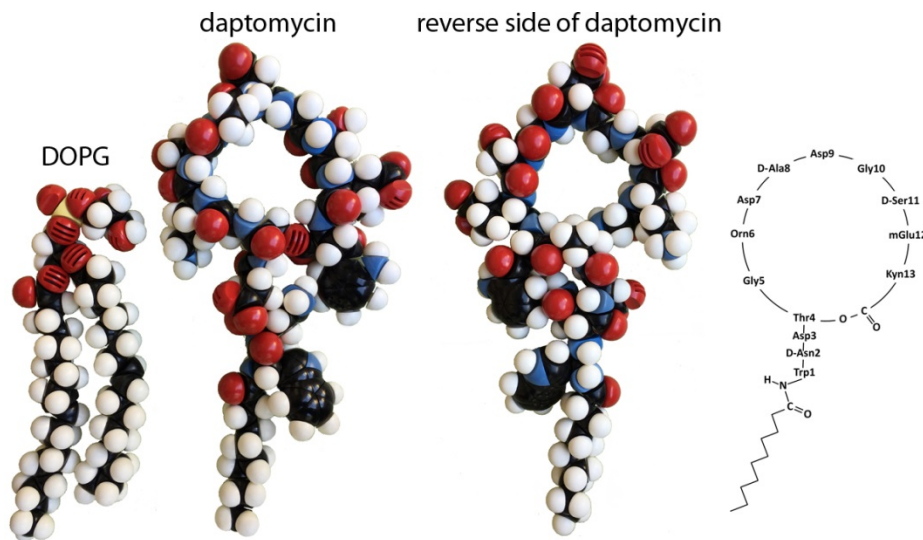


Fig. S3 CD spectra of daptomycin in different daptomycin/ Ca^{2+} /PG compositions. Shown here are the CD spectra of 40 μM daptomycin with 800 μM 7:3 DOPC/DOPG in 10 mM Tris buffer at pH 7.4 with Ca^{2+} concentrations between 0 and 103 μM . Each spectrum can be fit by a linear combination (dotted line) of two basis spectra A and B, with the percentage of B indicated. A is the CD with no Ca^{2+} ; B is the CD with 97 μM CaCl_2 . (Reproduced from ref. 26, Fig. 3)

